www.nature.com/aps

Acta Pharmacologica Sinica

ARTICLE

Establishment of an in vitro safety assessment model for lipid-lowering drugs using same-origin human pluripotent stem cell-derived cardiomyocytes and endothelial cells

Xuan Ni[1], Zhuang-zhuang Yang[1], Ling-qun Ye[1], Xing-long Han[1], Dan-dan Zhao[1], Feng-yue Ding[1], Nan Ding[1], Hong-chun Wu[1], Miao Yu[1], Guang-yin Xu[2], Zhen-ao Zhao[3], Wei Lei[1] and Shi-jun Hu[1]

Cardiovascular safety assessment is vital for drug development, yet human cardiovascular cell models are lacking. In vitro mass-generated human pluripotent stem cell (hPSC)-derived cardiovascular cells are a suitable cell model for preclinical cardiovascular safety evaluations. In this study, we established a preclinical toxicology model using same-origin hPSC-differentiated cardiomyocytes (hPSC-CMs) and endothelial cells (hPSC-ECs). For validation of this cell model, alirocumab, a human antibody against proprotein convertase subtilisin kexin type 9 (PCSK9), was selected as an emerging safe lipid-lowering drug; atorvastatin, a common statin (the most effective type of lipid-lowering drug), was used as a drug with reported side effects at high concentrations, while doxorubicin was chosen as a positive cardiotoxic drug. The cytotoxicity of these drugs was assessed using CCK8, ATP, and lactate dehydrogenase release assays at 24, 48, and 72 h. The influences of these drugs on cardiomyocyte electrophysiology were detected using the patch-clamp technique, while their effects on endothelial function were determined by tube formation and DiI-acetylated low-density lipoprotein (DiI-Ac-LDL) uptake assays. We showed that alirocumab did not affect the cell viability or cardiomyocyte electrophysiology in agreement with the clinical results. Atorvastatin (5–50 μM) dose-dependently decreased cardiovascular cell viability over time, and at a high concentration (50 μM, ~100 times the normal peak serum concentration in clinic), it affected the action potentials of hPSC-CMs and damaged tube formation and DiI-Ac-LDL uptake of hPSC-ECs. The results demonstrate that the established same-origin hPSC-derived cardiovascular cell model can be used to evaluate lipid-lowering drug safety in cardiovascular cells and allow highly accurate preclinical assessment of potential drugs.

Keywords: pluripotent stem cells; cardiomyocytes; endothelial cells; drug safety; lipid-lowering drugs; alirocumab; atorvastatin; doxorubicin

Acta Pharmacologica Sinica (2022) 43:240–250; https://doi.org/10.1038/s41401-021-00621-8

INTRODUCTION

The fields of cardiovascular safety and pharmacology have an important role in preclinical toxicity assessments to better guide drug development. Animal models are traditionally used for preclinical drug evaluation and inaccurately predict human cardiac pathophysiology due to interspecies differences in cardiac physiology [1, 2]. Cells transfected with the human ether-à-go-go-related gene (hERG) potassium channel are commonly utilized in drug-induced alterations in cardiac electrophysiology in vitro and often lead to a high rate of false-positive results [3, 4]. Primary human cardiovascular cells, the gold standard for assessing cardiovascular toxicity of drugs, are difficult to obtain and maintain. Thus, there is a considerable need to develop alternative human cardiovascular cell models. With significant methodological advances, human cardiomyocytes or endothelial cells can be mass-produced in vitro from human pluripotent stem cells (hPSCs), including human induced pluripotent stem cells (hiPSCs) and embryonic stem cells (hESCs), which provide a promising preclinical platform for drug evaluation [5–8].

Proprotein convertase subtilisin kexin type 9 (PCSK9) regulates cholesterol and/or lipid homeostasis by promoting low-density lipoprotein (LDL) receptor degradation and reducing LDL cholesterol clearance [9, 10]. PCSK9 has emerged as a promising lipid-lowering target for treating hypercholesterolemia and coronary heart disease [11], and PCSK9 inhibitors have successfully reduced the occurrence of hypercholesterolemia, coronary heart disease, and atherosclerotic cardiovascular disease [12]. However, no PCSK9 small molecule is currently in clinical development. Recently, the fully human anti-PCSK9 monoclonal antibodies alirocumab (Praluent) and evolocumab (Repatha) have been approved by the US Food and Drug Administration (FDA) to treat patients with hypercholesterolemia and mixed dyslipidemia [13]. Alirocumab, the first approved PCSK9 inhibitor, is safe and effective in reducing the LDL cholesterol level, with

[1]Department of Cardiovascular Surgery of the First Affiliated Hospital & Institute for Cardiovascular Science, Collaborative Innovation Center of Hematology, State Key Laboratory of Radiation Medicine and Protection, Medical College, Soochow University, Suzhou 215000, China; [2]Institute of Neuroscience, Soochow University, Suzhou 215123, China and [3]Institute of Microcirculation, Department of Pathophysiology of Basic Medical College, Hebei North University, Zhangjiakou 075000, China
Correspondence: Shi-jun Hu (shijunhu@suda.edu.cn)

Received: 25 July 2020 Accepted: 1 February 2021
Published online: 8 March 2021

some side effects that are primarily associated with injection-site reactions [14].

Similar to the PCSK9 inhibitors, 3-hydroxy-3-methylglutaryl-coenzyme A reductase inhibitors (statins) are among the most common lipid-lowering drugs for reducing LDL cholesterol and preventing cardiovascular events. However, some statin-treated patients have inadequate reductions in their LDL cholesterol level or non-LDL-related dyslipidemia, resulting in an elevated cardiovascular risk [10]. Furthermore, the side effects of statins include rhabdomyolysis and liver and renal toxicity [15, 16]. Thus, the adverse effects of statins may limit their tolerability and the ability to attain effective doses in some patients. Atorvastatin, a common lipophilic statin, is the most prescribed statin and has been widely used for the treatment of hypercholesterolemia and hypertriglyceridemia. However, the use of atorvastatin has now been limited because of several acute and chronic side effects observed in some cases with reports of causing hepatotoxicity, nephrotoxicity, and cardiac toxicity at high concentrations [17–20].

Doxorubicin is an effective anticancer anthracycline used in treating solid tumors and hematologic malignancies [21]. However, the clinical use of doxorubicin has been hampered because it causes dose-dependent cardiotoxicity in a subset of patients, which may result in the development of life-threatening cardiomyopathy [22, 23]. In mice, doxorubicin can induce endothelial and cardiomyocyte damage, mimicking doxorubicin-induced cardiotoxicity in the clinic [24]. The cardiotoxicity-associated mechanism of doxorubicin has been widely studied, but doxorubicin-induced mitochondrial dysfunction may be the most important potential mechanism of doxorubicin-related cardiotoxicity [25, 26]. At present, doxorubicin is the most commonly reported drug causing cardiotoxicity in many cardiovascular cell models [22, 27, 28].

To date, there have been no published studies of lipid-lowering drug-related preclinical models based on human pluripotent stem cell-derived cardiovascular cells. Our study aimed to develop a lipid-lowering drug-related preclinical model based on same-origin hPSC-induced cardiomyocytes (hPSC-CMs) and endothelial cells (hPSC-ECs). On this platform, we successfully performed cardiovascular toxicity assessment of three drugs, including alirocumab, atorvastatin and doxorubicin, and revealed the safety of alirocumab on cardiovascular cell viability and function.

MATERIALS AND METHODS

Maintenance of hESCs and hiPSCs

Human iPSCs and the ESC line H1 were routinely maintained in PSCeasy® medium (Cellapy, China) on Matrigel-coated plates as previously described [29, 30]. The hPSC lines were passaged every 3-4 days with 0.5 mM EDTA. To prevent dissociation-induced apoptosis of hPSCs, 2 μM thiazovivin (Selleck Chemicals, USA), a rho-associated protein kinase (ROCK) inhibitor, was added to the culture medium on the first day after cell passage. All cell cultures were maintained in a humidified incubator at 37 °C with an atmosphere of 5% CO_2.

Embryoid body (EB) formation

EB formation was used to test the in vitro differentiation ability of hiPSCs and hESCs. hPSCs were dissociated with EDTA and then cultured in DMEM/F12 supplemented with 20% knockout serum replacement (Thermo Fisher, USA), 2 mM *L*-glutamine, and 100 μM nonessential amino acids for 7 days on an ultralow-attachment six-well plate. EBs were collected and replated on a 0.1% gelatin-coated 35-mm dish. Then, after culturing for another 7 days, the cells were fixed with 4% paraformaldehyde (PFA) and stained with the indicated antibodies to detect endodermal (SOX17), mesodermal (α-SMA), and ectodermal (TUJ1) markers. The antibodies used for immunofluorescence staining are listed in Table S1.

Cardiomyocyte differentiation

Cardiomyocyte differentiation from hPSCs was performed according to a previously optimized protocol described by our laboratory [31]. Briefly, hiPSCs and hESCs were grown on Matrigel-coated 35-mm dishes until reaching 80%–90% confluence before cardiomyocyte differentiation was initiated. On day 0, the medium was changed to CDM3, which consisted of RPMI-1640 (Thermo Fisher, USA), bovine serum albumin (BSA; Sigma-Aldrich, USA), and *L*-ascorbic acid (Sigma-Aldrich, USA). Cells were first treated with 6 μM CHIR99021 (Sigma-Aldrich, USA) for 48 h. On day 2, the medium was changed to CDM3 supplemented with 2 μM Wnt-C59 (Selleck Chemicals, USA). Beginning on day 4, the medium was refreshed with CDM3 every 2 days, and spontaneously contracting cardiomyocytes were noted until day 7. Between days 10 and 14, the differentiated cells were cultured in glucose-free RPMI-1640 (Thermo Fisher, USA) containing BSA and *L*-ascorbic acid, as well as 5 mM sodium *DL*-lactate (Sigma-Aldrich, USA) for metabolic selection to remove noncardiomyocytes. The remaining cardiomyocytes were cultured for another 16 days and used for further study on day 30.

Endothelial cell differentiation

Human iPSCs and the ESC line H1 were differentiated into endothelial cells using a 2D monolayer differentiation protocol as previously described with some modifications [7]. Stem cells were grown to 95%–100% confluence on Matrigel-coated 35-mm dishes, and then refreshed with CDM3 containing 6 μM CHIR99021 for 48 h. Cells were subsequently cultured in CDM3 supplemented with 25 ng/mL basic fibroblast growth factor for 24 h and CDM3 supplemented with 50 ng/mL vascular endothelial growth factor and 25 ng/mL bone morphogenetic protein 4 for 3 days. The $CD144^+$ endothelial cells were then isolated by magnetic-activated cell sorting and maintained in endothelial growth medium-2 (Lonza, Switzerland) on gelatin-coated plates.

Alkaline phosphatase staining

Human iPSCs or ESCs were plated onto Matrigel-coated 35-mm dishes and cultured in PSCeasy® medium (Cellapy, China). When the confluence reached 60%–70%, the colonies were fixed and stained with a BCIP/NBT Alkaline Phosphatase Color Development Kit according to the manufacturer's instructions (Beyotime, China). Images of the stained colonies were acquired using an Olympus fluorescence microscope (Olympus, Japan).

Real-time quantitative PCR (RT-qPCR)

The cells were lysed with TRIzol Reagent® (Sigma-Aldrich, USA), and total RNA was isolated according to the manufacturer's instructions. Then, cDNA was synthesized from 500 ng of total RNA with a TaKaRa PrimeScript™ RT Reagent Kit (TaKaRa, Japan), and RT-qPCR was performed by using SYBR® Premix Ex Taq™ II (TaKaRa, Japan) in an Applied Biosystems StepOnePlus™ instrument (Thermo Fisher, USA). The mRNA expression levels were measured in triplicate samples and normalized to the endogenous reference gene *18S*. The comparative threshold cycle ($2^{-\Delta\Delta Ct}$) method was used for data analysis as previously described [32]. The primer sequences used for RT-qPCR are listed in Table S2.

Immunofluorescence staining

Cultured cells were fixed with 4% PFA for 15 min, permeabilized with 0.25% Triton X-100 in phosphate-buffered saline (PBS) for 15 min, and then blocked with 5% BSA in PBS for 60 min at room temperature. The cells were subsequently incubated overnight at 4 °C with primary antibodies, washed with PBS-T (0.1% Tween 20 in PBS), and then incubated with the appropriate secondary antibodies for 60 min and counterstained with Hoechst 33342 for 10 min at room temperature in the dark to visualize the cell nuclei. Immunostaining was examined with an LSM880 Zeiss confocal

microscope (Carl Zeiss, Germany). The antibodies used for immunofluorescence staining are listed in Table S1.

PCSK9 concentration assay

The PCSK9 levels in HepG2 cell extracts or supernatant were measured using a Human PCSK9 SimpleStep ELISA® Kit (Abcam, USA) following the manufacturer's instructions. PCSK9 secretion in each well of a 12-well plate was measured after adding exogenous PCSK9 (4 ng/mL; Abcam, USA) together with alirocumab (0.01, 0.1, or 0.5 μM; TeraMabs, China) or the PCSK9 inhibitor R-IMPP (10 μM; Sigma-Aldrich, USA).

Flow cytometry analysis

The cells were collected and then fixed with 1% PFA for 20 min and 90% cold methanol for 15 min, respectively. After incubating with 0.5% BSA in PBS for 15 min, the cells were incubated with primary antibodies for 1 h at room temperature, followed by incubation with the appropriate secondary antibodies at room temperature for 30 min. Then, the cells were rinsed three times with PBS and assayed using a Guava easyCyte™ 8 flow cytometer (EMD Millipore, Germany). The antibodies used for flow cytometry analysis are listed in Table S1.

Electrophysiology

Whole-cell action potentials (APs) of cardiomyocytes were recorded in current clamp mode using an Axopatch 200B Microelectrode Amplifier (Axon, USA), as previously reported [33]. Cultured hPSC-CMs were dissociated and plated as single cells on Matrigel-coated glass cover slips for 3 days. For whole-cell recordings, cells were incubated in an extracellular solution containing (in mM) 140 NaC1, 4 KCl, 1.2 $CaCl_2$, 1.0 $MgCl_2$, 10 HEPES, and 10 glucose, with the pH adjusted to 7.4 with NaOH. Pipette was filled with the intracellular solution consisting of (in mM) 115 potassium aspartate, 15 KCl, 4 NaC1 1.0 $MgCl_2$, 5 Mg-ATP, 5 HEPES, and 5 EGTA, with the pH was adjusted to 7.2 with KOH. APs were analyzed with pClamp 10.3 (Axon Instruments) and Clampfit 10.3 software to determine the AP duration at 90% repolarization (APD_{90}) and AP amplitude (APA) values. To evaluate whether alirocumab, atorvastatin, or doxorubicin affected the electrophysiology of cardiomyocytes, the cells were treated with drugs for 24 and 72 h before patching.

Tube formation assay

Fifty microliters of Matrigel was plated in each well of 96-well plates and incubated for 30 min at 37 °C. Then, 2×10^4 endothelial cells were seeded in each well, and the formation of vascular tubes was observed under a phase contrast microscope. To examine the effect of drugs on endothelial tube formation, endothelial cells were incubated with alirocumab, atorvastatin, or doxorubicin for 24 and 72 h before capturing images of the formed tubes.

Dil-acetylated LDL (Dil-Ac-LDL) uptake

Endothelial cells were seeded on 12-well plates at a density of 1×10^5 cells per well and grown to 80%–90% confluence. Then, 20 μg/mL Dil-Ac-LDL (Yeasen Biotech, China) was added, and the cells were incubated at 37 °C in the dark for an additional 4 h before being washed three times with PBS and imaged under a microscope. For the drug study, endothelial cells were incubated with alirocumab, atorvastatin, and doxorubicin for 24 and 72 h. Then, 20 μg/mL Dil-Ac-LDL was added for 4 h, and the cells were analyzed by a fluorescence microscope or flow cytometry. Dil-Ac-LDL uptake is expressed as the relative percentage of the geometric mean fluorescence intensity.

Quantitative viability assays

Human PSC-CMs between day 30 and day 40 or hPSC-ECs between day 10 and day 20, as well as the cardiomyocyte line H9C2 and human umbilical vein endothelial cells (HUVECs), were used for cell viability assays. The analyses were performed 24, 48, or 72 h after drug exposure. The concentrations of alirocumab were set at 0.01, 0.1, 1, 2, and 10 μM (that is 0.1, 1, 10, 20, and 100 times the peak serum concentration of 15 μg/mL), while the concentrations of atorvastatin were set at 0.05, 0.5, 5, 10, and 50 μM (0.1, 1, 10, 20, and 100 times the peak serum concentration of 252 ng/mL) [34, 35]. Five different doses of doxorubicin (0.1, 0.5, 1, 5, and 10 μM), as a positive control cardiotoxic drug, were used according to previous studies for doxorubicin toxicity analysis [28, 36]. The cell viability, ATP production, and intracellular lactate dehydrogenase (LDH) activity were evaluated by using the Cell Counting Kit 8 (CCK8) Assay (Dojindo, Japan), CellTiter-Glo Viability Assay (Promega, USA), and CytoTox-ONE™ Homogeneous Membrane Integrity Assay (Promega, USA) kits, respectively, according to the manufacturer-recommended procedures. Viability measurements were conducted using a microplate reader (BioTek, USA).

Statistical analysis

Comparisons between two groups were analyzed with Student's *t* test. Comparisons of multiple groups were performed using one-way analysis of variance post hoc test. At least three replicates were performed per experiment. All data are presented as the mean ± SD. Differences with P values < 0.05 were considered significant.

RESULTS

Establishment of a cardiovascular cell model

To develop a human cardiovascular cell model for drug safety evaluation, hiPSCs were initially obtained by reprogramming human fibroblasts and were then confirmed to have morphological characteristics similar to those of hESCs, including bright edges and a high nuclear-cytoplasmic ratio (Fig. S1a). In addition, hiPSCs and hESCs exhibited comparable expression of pluripotent stem cell markers (OCT-3/4, SOX2, and NANOG) (Fig. 1a, b), similar alkaline phosphatase activity (Fig. S1b), and the same capacity to differentiate into cells from all three germ layers (Fig. S1c). Both the hiPSC and hESC lines used in this study had normal karyotypes (Fig. S1d).

Using direct differentiation protocols, both hiPSCs and hESCs were successfully differentiated into synchronously beating cardiomyocytes (hiPSC-CMs and hESC-CMs) (Fig. 1c–e, Movies S1 and S2) and endothelial cells (hiPSC-ECs and hESC-ECs) (Fig. 1f–i). Flow cytometry analysis showed that the percentages of cardiac troponin T (TNNT2)-positive cardiomyocytes reached over 90% in both hiPSC- and hESC-derived cell populations (Fig. 1c). Moreover, the TNNT2 staining data showed that the differentiated cardiomyocytes had a normal myofilament structure (Fig. 1d). The hiPSC-CMs and hESC-CMs presented their electrophysiological properties (Fig. 1e) as determined by the patch-clamp technique. Regarding endothelial cells, the purities of CD31 and CD144 double-positive hiPSC-ECs and hESC-ECs were greater than 90% after MACS-based cell purification (Fig. 1f). The immunofluorescence staining results further confirmed the visual expression of CD144 in the purified hiPSC-ECs and hESC-ECs (Fig. 1g). In addition, these cells exhibited an in vitro angiogenesis potential as indicated by their tube formation (Fig. 1h) and Dil-Ac-LDL uptake abilities (Fig. 1i). The tube branching and LDL uptake abilities were not significantly different between hiPSC-ECs and hESC-ECs. Therefore, the above data indicated that functional cardiovascular cells were successfully induced from hPSCs.

Cardiomyocyte-related cytotoxicity assessments

We selected the monoclonal antibody alirocumab as a representative anti-PCSK9 drug for lipid-lowering drug-related preclinical drug assessment. Alirocumab was safe (Fig. S2a) and effective in inhibiting PCSK9 secretion in HepG2 cells by reducing the

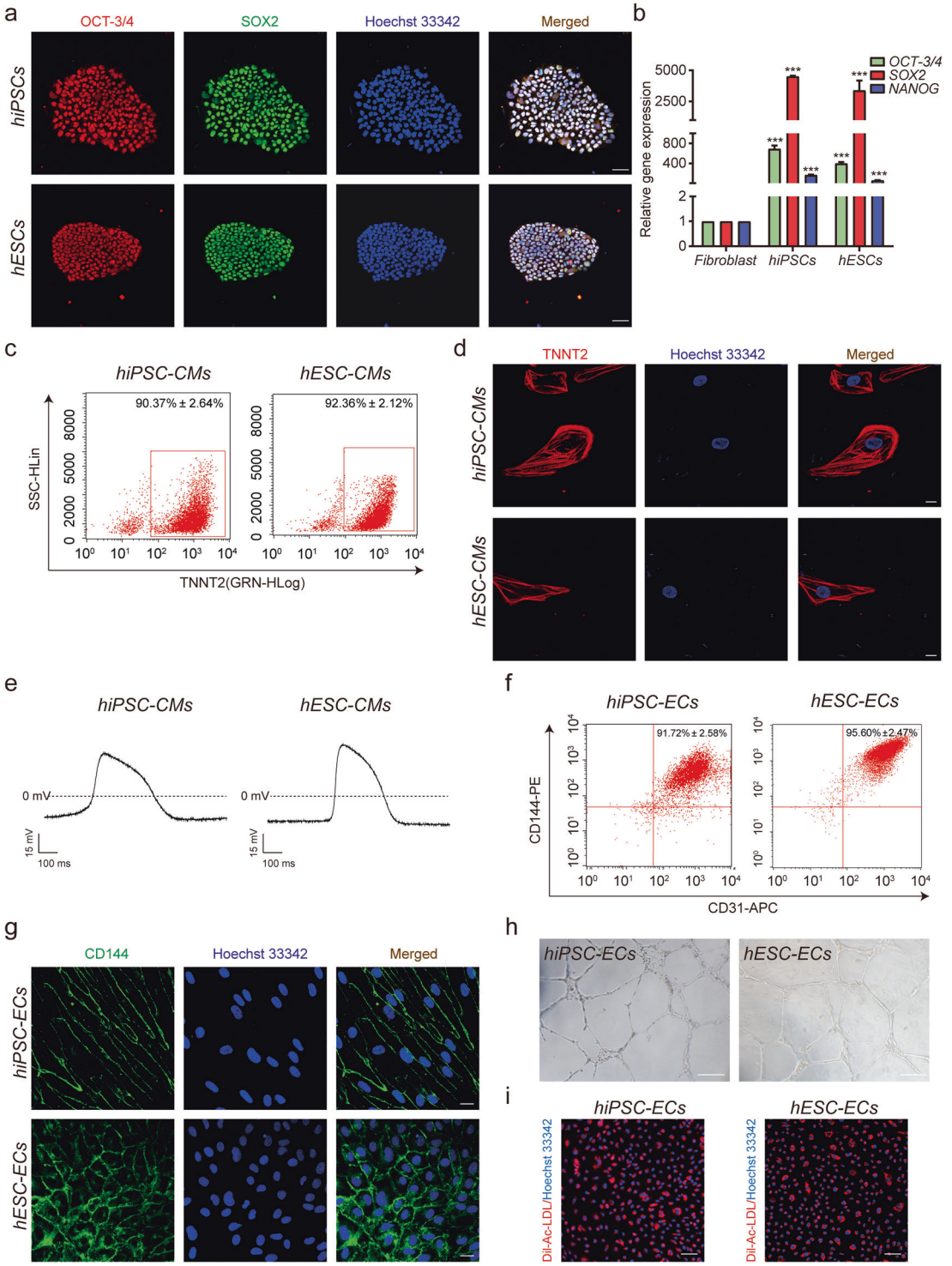

Fig. 1 Characterization of undifferentiated hPSCs (hiPSCs and hESCs) and their derived cardiovascular cells. a Immunofluorescence staining of pluripotency proteins OCT-3/4 (red) and SOX2 (green) in undifferentiated hiPSCs and hESCs. Nuclei were labeled with Hoechst 33342 (blue). Scale bar, 50 μm. **b** Gene expression levels of pluripotency markers (*OCT-3/4, SOX2*, and *NANOG*) in hiPSCs and hESCs compared with fibroblasts ($n = 3$). **c** Flow cytometry analysis of the cardiac structural marker troponin T (TNNT2)-positive cells in hPSC-derived cells after cardiomyocyte differentiation. **d** Immunofluorescence staining of hPSC-CMs for TNNT2 (red). Nuclei were stained with Hoechst 33342 (blue). Scale bar, 10 μm. **e** Typical cardiomyocyte waveforms were acquired in hPSC-CMs by the patch-clamp technique. **f** Flow cytometry analysis of CD31- and CD144-positive hPSC-ECs post cell purification. **g** Immunofluorescence images showing the expression of the endothelial marker CD144 (green). Nuclei were stained with Hoechst 33342 (blue). Scale bar, 20 μm. **h** Cord-like structure formation of hiPSC-ECs and hESC-ECs was visualized under a phase contrast microscope. Scale bar, 100 μm. **i** DiI-Ac-LDL uptake was observed in both hiPSC-ECs and hESC-ECs. Nuclei were stained with Hoechst 33342 (blue). Scale bar, 100 μm.

concentration of PCSK9 in HepG2 cell supernatants but not in cell extracts after the addition of exogenous PCSK9 (Fig. S2b). R-IMPP, an inhibitor of PCSK9 expression, was selected as a positive control, as it was demonstrated to significantly decrease the PCSK9 concentration in both HepG2 cell extracts and supernatants (Fig. S2b). Then, we performed independent cytotoxicity assays to evaluate the structural safety of alirocumab and atorvastatin on our hPSC-CM model, while doxorubicin was used as a positive cardiotoxic control. To test the dose-dependent effects, hiPSC-CMs and hESC-CMs were treated with alirocumab or atorvastatin at five different doses for 24, 48, and 72 h, respectively. The doses of alirocumab or atorvastatin were set to have the same multiples based on their peak serum concentrations. As expected, the positive cardiotoxic control doxorubicin showed dose-dependent cardiac damage in hiPSC-CMs and hESC-CMs at 24, 48, and 72 h, as assessed by a CCK8 assay (Fig. 2a). Following incubation with alirocumab at different concentrations (0.01, 0.1, 1, 2, and 10 μM), hiPSC-CMs and hESC-CMs exhibited normal cell viability, indicating that alirocumab was safe. Similar to doxorubicin, atorvastatin also induced dose-dependent cardiac damage in hPSC-CMs after 24, 48, and 72 h (Fig. 2a). ATP analysis results also verified the safety of alirocumab in hiPSC-CMs and hESC-CMs. However, the ATP levels were significantly reduced in hPSC-CMs treated with doxorubicin or atorvastatin at high doses (Fig. 2b), indicating that these two drugs resulted in energy impairment in these cells. Similar to the CCK8 and ATP assay results, the LDH release experiment showed that doxorubicin could induce LDH release after 24, 48, and 72 h, indicating that doxorubicin caused cell plasma membrane damage (Fig. 2c). However, alirocumab did not affect the level of LDH release in hiPSC-CMs and hESC-CMs. Atorvastatin was proven to have no effect on LDH release when applied for 24 h, even at 50 μM, but it led to significant LDH release in hPSC-CMs at high concentrations when administered for a longer period of time (48 and 72 h).

We next assessed the morphology of hPSC-CMs after drug treatment. We found that alirocumab (0.1–10 μM) and atorvastatin at a low concentration (0.5 μM) did not affect the cellular state of hiPSC-CMs at 24, 48, and 72 h, whereas the treatments with atorvastatin at high concentrations (5 and 50 μM) for 48 and 72 h or with 10 μM doxorubicin for 24, 48, and 72 h significantly impaired the cell morphology (Fig. S3). The changes in hiPSC-CM morphology after the indicated drug treatments were similar to those observed in hESC-CM (data not shown). Furthermore, we performed CCK8, ATP, and LDH assays in rat myocardial H9C2 cells, to assess the myocardial safety data of alirocumab, atorvastatin, and doxorubicin. The data obtained from H9C2 cells were similar to those obtained from hiPSC-CMs and hESC-CMs (Fig. S4).

Assessment of cardiomyocyte electrophysiology

To evaluate whether alirocumab and atorvastatin affected the electrophysiology of hPSC-CMs, we used the patch-clamp technique to assess the influence of these drugs on the APs of hiPSC-CMs and hESC-CMs after 24 and 72 h of treatment. The results showed that alirocumab did not affect the AP waveform of hiPSC-CMs and hESC-CMs at 24 and 72 h (Fig. 3a, c). Furthermore, the APD_{90} repolarization and APA values of the alirocumab group at 24 and 72 h were similar to those of the control group (Fig. 3b, d). Although 0.5 μM atorvastatin had no effect on the APD_{90} and APA values, 50 μM atorvastatin significantly induced APD_{90} prolongation of hiPSC-CMs and hESC-CMs after 24 and 72 h of treatment (Fig. 3). Atorvastatin (50 μM) reduced the APA value of hiPSC-CMs after 24 h of incubation, although it did not affect the APA value of hESC-CMs. Although its 24 h treatment did not affect APD_{90} and APA values of hiPSC-CMs and hESC-CMs, doxorubicin (10 μM) significantly reduced the APA value of hiPSC-CMs and hESC-CMs after 72 h of treatment. Moreover, 10 μM doxorubicin also reduced the APD_{90} value of hESC-CMs at 72 h, although the effect was not significant in hiPSC-CMs (Fig. 3).

Endothelial cell-related cytotoxicity evaluation

We next used the hPSC-EC model to evaluate the safety of alirocumab and atorvastatin. The CCK8 data showed that alirocumab treatment for 24, 48, and 72 h was safe in both hiPSC-ECs and hESC-ECs. Doxorubicin, a positive control cardiotoxic drug, significantly decreased cell viability of hPSC-ECs after 24 h of treatment, and its toxicity increased with increasing concentrations and time (48 and 72 h). After 24 h of incubation with a high concentration of atorvastatin (50 μM), the hPSC-EC viability was reduced, and toxicity was more notable with longer incubation time while lower concentrations of atorvastatin (5 and 10 μM) also affected hPSC-EC viability after 48 and 72 h of treatment (Fig. 4a). The ATP analysis results also verified these findings (Fig. 4b). Compared with the control treatment, alirocumab did not affect the ATP level, whereas doxorubicin led to low ATP concentrations. In the atorvastatin group, lower ATP levels in hiPSC-ECs and hESC-ECs were only noted at a high concentration (50 μM) after incubation for 24 h, but upon prolonged incubation (48 and 72 h), atorvastatin showed greater toxicity, even at lower concentrations (5 and 10 μM) (Fig. 4b). Both doxorubicin and atorvastatin increased LDH release when treated at high concentrations or when administered at low concentrations for a sustained period (Fig. 4c). Unlike doxorubicin and atorvastatin, alirocumab at both low and high concentrations did not affect the level of LDH release (Fig. 4c). The above cytotoxic results were similar to the data presented in Fig. 2 for hiPSC-CMs and hESC-CMs.

Moreover, we also observed the morphology of hPSC-ECs following drug treatment for 24, 48, and 72 h. In agreement with the cell viability data, alirocumab (0.1-10 μM) and 0.5 μM atorvastatin did not affect the morphology of hiPSC-ECs, while atorvastatin (50 μM) and doxorubicin (1 and 10 μM) affected endothelial cell morphology after 24 h of incubation and significantly worsened the morphology after 48 and 72 h of treatment (Fig. S5). The morphology of hESC-ECs after drug treatment was similar to the results of hiPSC-ECs (data not shown). When using HUVEC cell model, we observed similar cell viability results as those obtained from hiPSC-ECs and hESC-ECs (Fig. S6).

Evaluation of endothelial function

In addition to the cytotoxicity evaluations, the influence of alirocumab and atorvastatin on the function of hPSC-ECs was investigated. Tube formation assays were conducted after drug treatment with alirocumab (0.1, 1, and 10 μM), atorvastatin (0.5, 5, and 50 μM), or doxorubicin (1 and 10 μM). When placed on Matrigel, we observed that hPSC-ECs all formed intact tube-like structures after incubation with drugs. Through tube structure analyses, we found that 24 and 72 h of treatment with alirocumab (0.1, 1, and 10 μM) or 0.5 μM atorvastatin did not affect the formation of cord-like structures (Fig. 5a, b). However, the 50 μM atorvastatin and 10 μM doxorubicin treatments harmed the integrity of the tubes formed by hiPSC-ECs and hESC-ECs at 24 and 72 h, while the 5 μM atorvastatin and 1 μM doxorubicin treatments only damaged the integrity of the tubes of hPSC-ECs at 72 h (Fig. 5a, b). In addition, we investigated the effects of alirocumab and atorvastatin on Dil-Ac-LDL uptake by hPSC-ECs after 24 and 72 h of treatment. The results showed that alirocumab did not influence the Dil-Ac-LDL level in hiPSC-ECs or hESC-ECs (Fig. 5c, d). At a low concentration (0.5 μM), atorvastatin did not obviously affect the Dil-Ac-LDL uptake, while at higher concentrations (5 and 50 μM), it appeared to decrease the level of Dil-Ac-LDL uptake in both hiPSC-ECs and hESC-ECs (Fig. 5c, d), especially after 72 h of treatment. Flow cytometry also verified these results (Fig. S7). In addition, consistent with its toxicity to hPSC-EC viability and tube formation, doxorubicin at 1 and 10 μM also damaged the Dil-Ac-LDL uptake ability of hPSC-ECs (Fig. 5c, d). Taken together, these data suggested that alirocumab did not affect endothelial cell function, including tube

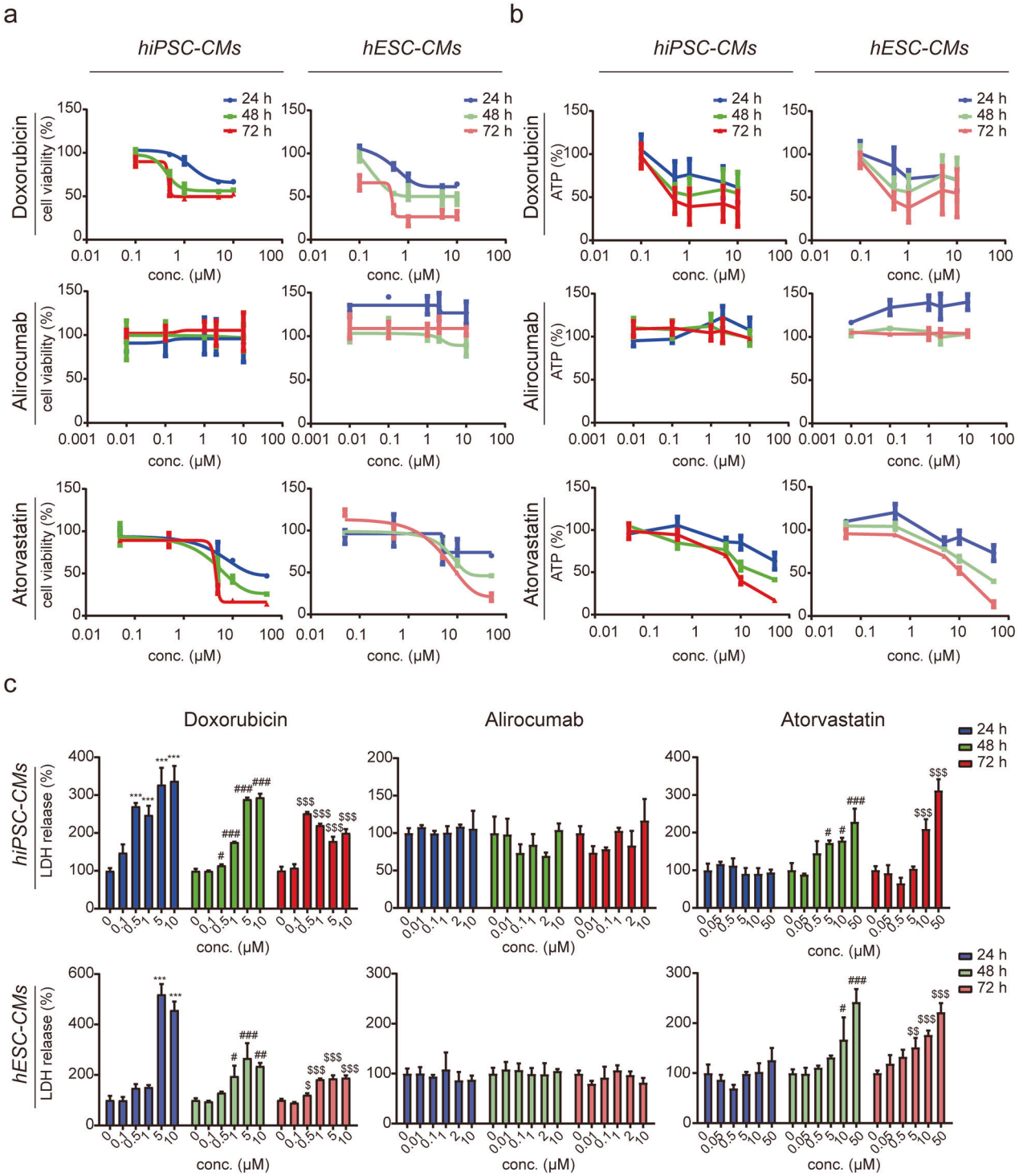

Fig. 2 Quantitative viability assessments of hiPSC-CMs and hESC-CMs. a CCK8 assay results for hiPSC-CMs and hESC-CMs after 24, 48, and 72 h of treatment with alirocumab (0.01, 0.1, 1, 2, and 10 μM) and atorvastatin (0.05, 0.5, 5, 10, and 50 μM). Doxorubicin (0.1, 0.5, 1, 5, and 10 μM) was used as a cardiotoxic positive control ($n \geq 3$). **b** ATP levels in hiPSC-CMs and hESC-CMs were measured after doxorubicin, alirocumab, and atorvastatin treatments ($n \geq 3$). **c** Lactate dehydrogenase (LDH) release levels were assessed in both hiPSC-CMs and hESC-CMs after 24, 48, and 72 h of treatment with doxorubicin, alirocumab, and atorvastatin ($n \geq 3$). ***$P < 0.001$ in the 24 h treatment group. $^{\#}P < 0.05$, $^{\#\#}P < 0.01$; $^{\#\#\#}P < 0.001$ in the 48 h treatment group. $^{\$}P < 0.05$; $^{\$\$}P < 0.01$; $^{\$\$\$}P < 0.001$ in the 72 h treatment group.

formation and Dil-Ac-LDL uptake, while atorvastatin at high concentrations (5 and 50 μM) and doxorubicin (1 and 10 μM) damaged endothelial cell function, especially over longer treatment time (72 h).

DISCUSSION

Terminally differentiated cells, such as adult cardiomyocytes and endothelial cells, are the most suited for high-throughput drug screening. Because of the scarcity of human primary

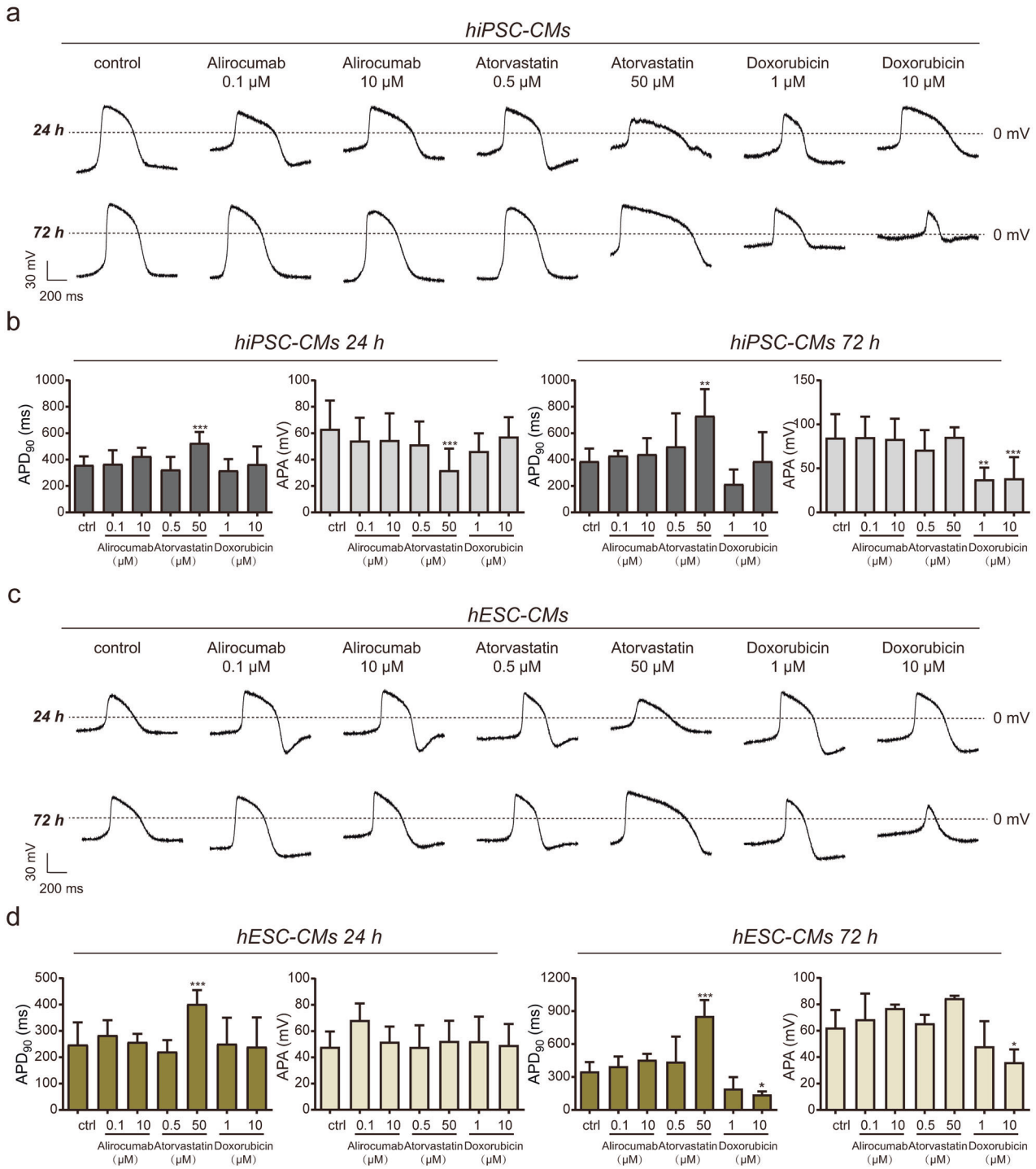

Fig. 3 Assessments of cardiomyocyte electrophysiology after drug treatment. a Cardiomyocyte waveforms were recorded in hiPSC-CMs after 24 and 72 h of drug treatment. Different concentrations of alirocumab (0.1 and 10 μM), atorvastatin (0.5 and 50 μM), and doxorubicin (1 and 10 μM) were evaluated. **b** APD_{90} (action potential duration at 90% repolarization) and APA (AP amplitude) values for hiPSC-CMs were calculated using Clampfit after drug treatment for 24 and 72 h ($n = 4$-16). $^{**}P < 0.01$; $^{***}P < 0.001$. **c** Cardiomyocyte waveforms were recorded in hESC-CMs after 24 and 72 h of treatment. The drugs were used at the following concentrations: alirocumab (0.1 and 10 μM), atorvastatin (0.5 and 50 μM), and doxorubicin (1 and 10 μM). **d** Statistical analyses of the APD_{90} and APA values in hESC-CMs after 24 and 72 h of treatment ($n = 4$-16). $^{*}P < 0.05$; $^{***}P < 0.001$.

cardiovascular cells, hPSC-derived cardiovascular cells show great promise for assessing the safety and efficacy of drugs on the heart. In particular, hiPSC-CMs are increasingly being used for disease modeling, drug discovery, and toxicity evaluation studies [37, 38]. For the first time, the results of our study showed the establishment of a valuable and reproducible in vitro cellular model based on same-origin human pluripotent stem cell-derived cardiovascular cells to study preclinical

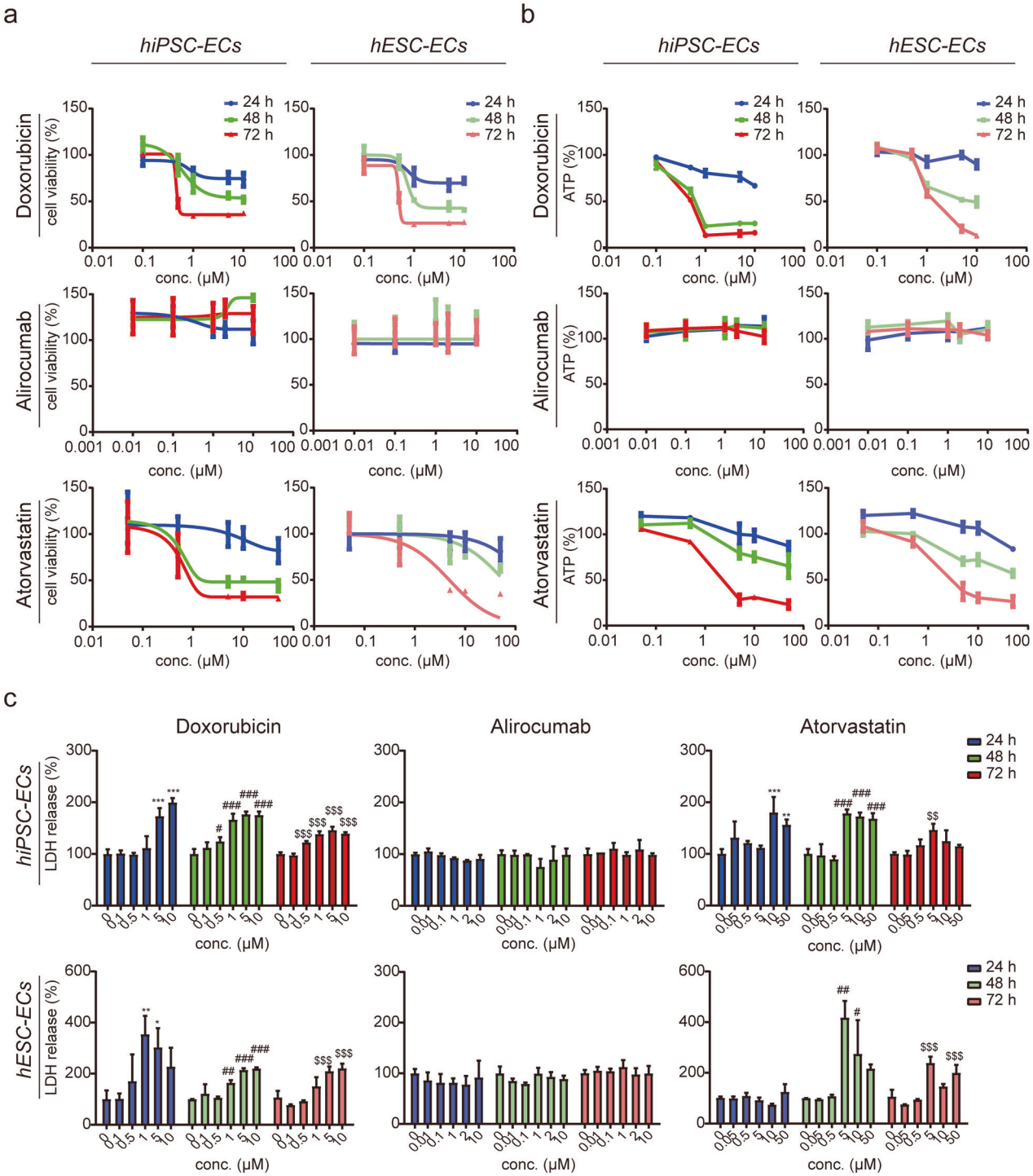

Fig. 4 Quantitative viability assessments of hiPSC-ECs and hESC-ECs. a CCK8 assay of hiPSC-ECs and hESC-ECs after 24, 48, and 72 h of treatment with alirocumab (0.01, 0.1, 1, 2, and 10 μM) and atorvastatin (0.05, 0.5, 5, 10, and 50 μM) at 24, 48, and 72 h. Doxorubicin (0.1, 0.5, 1, 5, and 10 μM) was used as a cardiotoxic positive drug ($n \geq 3$). **b** ATP levels of hiPSC-ECs and hESC-ECs incubated with different drugs (doxorubicin, alirocumab, and atorvastatin) for 24, 48, and 72 h were evaluated ($n \geq 3$). **c** LDH release from hiPSC-ECs and hESC-ECs was assessed after drug treatment for 24, 48, and 72 h ($n \geq 3$). $^{*}P < 0.05$; $^{**}P < 0.01$; $^{***}P < 0.001$ in the 24 h treatment group. $^{\#}P < 0.05$, $^{\#\#}P < 0.01$; $^{\#\#\#}P < 0.001$ in the 48 h treatment group. $^{\$\$}P < 0.01$; $^{\$\$\$}P < 0.001$ in the 72 h treatment group.

lipid-lowering drug safety. Furthermore, hPSC-CMs and hPSC-ECs can be obtained from both healthy individuals and patient- and disease-specific resources, which are the basis of diverse disease models for use in multilevel safety pharmacological screening. In addition, our model, a same-origin hPSC-derived cardiovascular cell model, may facilitate more accurate predictions of the responses to personalized medicine under the same genetic background. Thus, our model can not only facilitate the prediction of potential preclinical cardiotoxic drugs but may also become a specific model for personalized medicine.

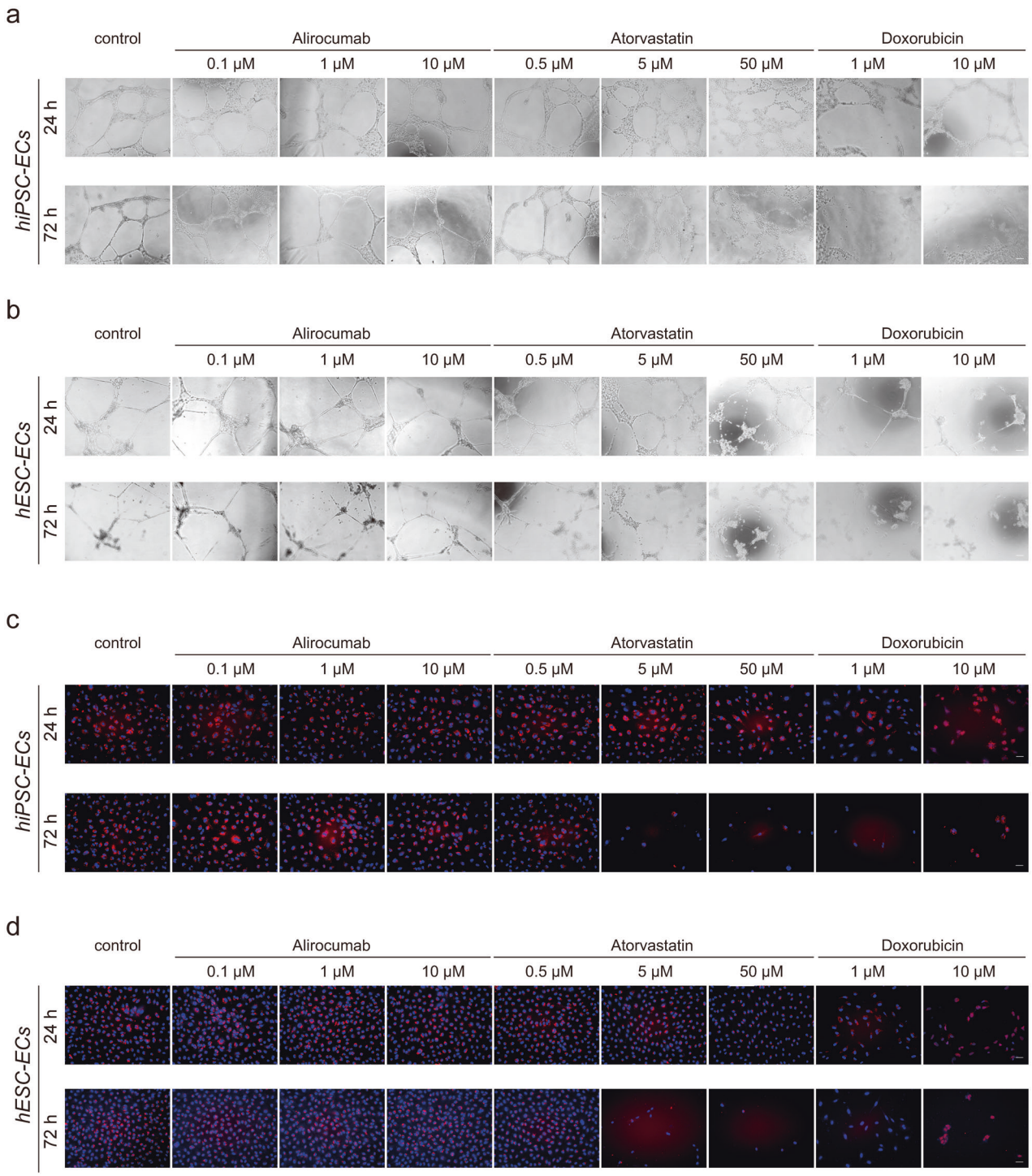

Fig. 5 Assessments of endothelial function after drug treatment. a Tube-like structures formed by hiPSC-ECs after 24 and 72 h of treatment. Different concentrations of alirocumab (0.1, 1, and 10 μM) and atorvastatin (0.5, 5, and 50 μM) as well as doxorubicin (1 and 10 μM) were used for assessments. Scale bar, 100 μm. **b** Images of tube-like structures formed by hESC-ECs after the indicated drug treatments for 24 and 72 h. Scale bar, 100 μm. **c** The Dil-Ac-LDL (red) uptake ability of hiPSC-ECs after alirocumab (0.1, 1, and 10 μM), atorvastatin (0.5, 5, and 50 μM), and doxorubicin (1 and 10 μM) treatments for 24 and 72 h. Nuclei were stained with Hoechst 33342 (blue). Scale bar, 50 μm. **d** The Dil-Ac-LDL (red) uptake ability of hESC-ECs after alirocumab, atorvastatin, and doxorubicin treatments for 24 and 72 h. Nuclei were stained with Hoechst 33342 (blue). Scale bar, 50 μm.

Doxorubicin, a chemotherapy drug that can lead to cardiotoxicity, has been widely used in hPSC-related drug evaluation models [28, 39, 40]. To assess whether hPSC-CMs and hPSC-ECs are both suitable for drug safety evaluation, we treated these cells with doxorubicin. Based on the results, both hPSC-CMs and hPSC-ECs can be used to accurately reproduce drug-induced toxicity in a dose-dependent manner, as was reported by Zhao et al. [39]. In our report, doxorubicin not only reduced cell viability but also affected cardiovascular cell (CMs and ECs) function. Thus, the above data indicated that our hPSC-derived cardiovascular cell

model was successful and suitable for the evaluation of other drugs including lipid-lowering drugs.

Alirocumab, the first PCSK9 inhibitor approved by the FDA and the European Medicines Agency, is currently recommended as a first-line lipid-lowering treatment for patients with familial hypercholesterolemia [41]. The most common adverse effects of alirocumab treatment are injection-site reactions, back pain, and fall, but no other specific safety issues or concerns have been noted [42]. Emerging data indicate that alirocumab is safe for human cardiovascular cells. However, because of high costs and some efficacy problems, PCSK9 antibody drugs are lacking, and patient use is limited. In agreement with the clinical data, alirocumab (even ~100 times the normal peak serum concentration in clinic) was indeed safe in our model. Therefore, our model may aid in promoting PCSK9-related drug development by allowing for preclinical safety evaluations using human cardiovascular cells.

Statins are widely used as lipid-lowering agents, and the side effects of most statins have been reported to be related to hepatorenal and muscular toxicities [43, 44]. Furthermore, the side effects of statins are regarded as dose-related, and they can disappear upon the withdrawal of statin drugs [45]. Atorvastatin, a highly effective statin for treating hypercholesterolemia and hypertriglyceridemia, is generally thought to be safe and effective without the potential for abuse. However, atorvastatin use is restricted due to several acute and chronic side effects [46–48]. At the cellular level, high concentrations of atorvastatin (25, 50, 75, 100, and 125 μM) have been reported to be toxic toward mitochondria in the pancreas by reducing ATP level and increasing mitochondrial swelling [46]. In addition, high concentrations of atorvastatin have been reported to be cardiotoxic (more than 80 mg daily) [19] and to induce endothelial damage [20], while low concentrations have a protective effect against cardiovascular diseases [49]. In our study, atorvastatin was nontoxic for hPSC-CMs at low concentrations, as it has been reported that atorvastatin at low concentrations has no influence on the cell viability or contractile properties of hiPSC-CMs [50]. However, our results also suggested that atorvastatin was toxic to both hPSC-CMs and hPSC-ECs at a high concentration (50 μM, ~100 times normal peak serum concentration in clinic), especially with longer incubation time (48 and 72 h). Finally, our data demonstrated that 50 μM atorvastatin also promoted AP prolongation, which is similar to the results of a report indicating that atorvastatin inhibits the hERG current, suggesting that it may prolong the duration of AP [51].

In summary, in this study, we successfully established a human cardiovascular cell model for the preclinical assessment of different aspects of lipid-lowering drugs. In the future, hPSC-derived cardiovascular cell models, especially patient-specific cell models, will be used to screen more drugs for safety and to promote individualized lipid-lowering drug development.

ACKNOWLEDGEMENTS

This work was funded by the National Key R&D Program of China (2017YFA0103700), the National Natural Science Foundation of China (91949111, 81770257, and 81970223), the Natural Science Foundation of Jiangsu Province (BK20201409), Top Six Talents in Jiangsu Province (SWYY-081), Jiangsu Province's Key Discipline/Laboratory of Medicine (XK201118), the National Center for International Research (2017B01012), and the Introduction Project of Clinical Medicine Expert Team for Suzhou (SZYJTD201704)

AUTHOR CONTRIBUTIONS

XN designed the study, performed the experiments, and wrote the manuscript. SJH, WL, ZAZ, and GYX were responsible for designing the experiments and reviewing the manuscript. ZZY and FYD were involved in endothelial cell induction and verification. LQY, XLH, DDZ, and ND took part in hPSC-derived cardiomyocyte differentiation. MY and HCW provided technical assistance.

ADDITIONAL INFORMATION

Supplementary information The online version contains supplementary material available at https://doi.org/10.1038/s41401-021-00621-8.

Competing interests: The authors declare no competing interests.

REFERENCES

1. Magdy T, Schuldt AJT, Wu JC, Bernstein D, Burridge PW. Human induced pluripotent stem cell (hiPSC)-derived cells to assess drug cardiotoxicity: opportunities and problems. Annu Rev Pharmacol Toxicol. 2018;58:83–103.
2. Paik DT, Chandy M, Wu JC. Patient and disease-specific induced pluripotent stem cells for discovery of personalized cardiovascular drugs and therapeutics. Pharmacol Rev. 2020;72:320–42.
3. Sharma A, McKeithan WL, Serrano R, Kitani T, Burridge PW, Del Alamo JC, et al. Use of human induced pluripotent stem cell-derived cardiomyocytes to assess drug cardiotoxicity. Nat Protoc. 2018;13:3018–41.
4. Mercola M, Colas A, Willems E. Induced pluripotent stem cells in cardiovascular drug discovery. Circ Res. 2013;112:534–48.
5. Ivashchenko CY. Human embryonic and induced pluripotent stem cells in cardiovascular drug discovery: patents and patented uses. Recent Pat Cardiovasc Drug Discov. 2011;6:199–206.
6. Burridge PW, Matsa E, Shukla P, Lin ZC, Churko JM, Ebert AD, et al. Chemically defined generation of human cardiomyocytes. Nat Methods. 2014;11:855–60.
7. Hu S, Zhao MT, Jahanbani F, Shao NY, Lee WH, Chen H, et al. Effects of cellular origin on differentiation of human induced pluripotent stem cell-derived endothelial cells. JCI Insight. 2016;1:e85558.
8. Sriram G, Tan JY, Islam I, Rufaihah AJ, Cao T. Efficient differentiation of human embryonic stem cells to arterial and venous endothelial cells under feeder- and serum-free conditions. Stem Cell Res Ther. 2015;6:261.
9. Seidah NG, Awan Z, Chretien M, Mbikay M. PCSK9: a key modulator of cardiovascular health. Circ Res. 2014;114:1022–36.
10. Hess CN, Low Wang CC, Hiatt WR. PCSK9 inhibitors: mechanisms of action, metabolic effects, and clinical outcomes. Annu Rev Med. 2018;69:133–45.
11. Zhang L, McCabe T, Condra JH, Ni YG, Peterson LB, Wang W, et al. An anti-PCSK9 antibody reduces LDL-cholesterol on top of a statin and suppresses hepatocyte SREBP-regulated genes. Int J Biol Sci. 2012;8:310–27.
12. Gallego-Colon E, Daum A, Yosefy C. Statins and PCSK9 inhibitors: a new lipid-lowering therapy. Eur J Pharmacol. 2020;878:173114.
13. Reiss AB, Shah N, Muhieddine D, Zhen J, Yudkevich J, Kasselman LJ, et al. PCSK9 in cholesterol metabolism: from bench to bedside. Clin Sci. 2018;132:1135–53.
14. Robinson JG, Farnier M, Krempf M, Bergeron J, Luc G, Averna M, et al. Efficacy and safety of alirocumab in reducing lipids and cardiovascular events. N Engl J Med. 2015;372:1489–99.
15. Bjornsson ES. Hepatotoxicity of statins and other lipid-lowering agents. Liver Int. 2017;37:173–8.
16. Kitzmiller JP, Mikulik EB, Dauki AM, Murkherjee C, Luzum JA. Pharmacogenomics of statins: understanding susceptibility to adverse effects. Pharmgenomics Pers Med. 2016;9:97–106.
17. Pal S, Ghosh M, Ghosh S, Bhattacharyya S, Sil PC. Atorvastatin induced hepatic oxidative stress and apoptotic damage via MAPKs, mitochondria, calpain and caspase12 dependent pathways. Food Chem Toxicol. 2015;83:36–47.
18. Hasanpour Z, Nasri H, Rafieian-Kopaei M, Ahmadi A, Baradaran A, Nasri P, et al. Paradoxical effects of atorvastatin on renal tubular cells: an experimental investigation. Iran J Kidney Dis. 2015;9:215–20.
19. Caner M, Sonmez B, Kurnaz O, Aldemir C, Salar S, Altug T, et al. Atorvastatin has cardiac safety at intensive cholesterol-reducing protocols for long term, yet its cancer-treatment doses with chemotherapy may cause cardiomyopathy even under coenzyme-Q10 protection. Cell Biochem Funct. 2007;25:463–72.
20. Broniarek I, Jarmuszkiewicz W. Atorvastatin affects negatively respiratory function of isolated endothelial mitochondria. Arch Biochem Biophys. 2018;637:64–72.
21. Li M, Sala V, De Santis MC, Cimino J, Cappello P, Pianca N, et al. Phosphoinositide 3-kinase gamma inhibition protects from anthracycline cardiotoxicity and reduces tumor growth. Circulation. 2018;138:696–711.
22. Burridge PW, Li YF, Matsa E, Wu H, Ong SG, Sharma A, et al. Human induced pluripotent stem cell-derived cardiomyocytes recapitulate the predilection of breast cancer patients to doxorubicin-induced cardiotoxicity. Nat Med. 2016;22:547–56.
23. Carvalho FS, Burgeiro A, Garcia R, Moreno AJ, Carvalho RA, Oliveira PJ. Doxorubicin-induced cardiotoxicity: from bioenergetic failure and cell death to cardiomyopathy. Med Res Rev. 2014;34:106–35.
24. Rasanen M, Degerman J, Nissinen TA, Miinalainen I, Kerkela R, Siltanen A, et al. VEGF-B gene therapy inhibits doxorubicin-induced cardiotoxicity by endothelial protection. Proc Natl Acad Sci USA. 2016;113:13144–9.

25. Pereira GC, Silva AM, Diogo CV, Carvalho FS, Monteiro P, Oliveira PJ. Drug-induced cardiac mitochondrial toxicity and protection: from doxorubicin to carvedilol. Curr Pharm Des. 2011;17:2113–29.
26. Dolinsky VW. The role of sirtuins in mitochondrial function and doxorubicin-induced cardiac dysfunction. Biol Chem. 2017;398:955–74.
27. Weng KC, Kurokawa YK, Hajek BS, Paladin JA, Shirure VS, George SC. Human induced pluripotent stem-cardiac-endothelial-tumor-on-a-chip to assess anticancer efficacy and cardiotoxicity. Tissue Eng Part C Methods. 2020;26:44–55.
28. Maillet A, Tan K, Chai X, Sadananda SN, Mehta A, Ooi J, et al. Modeling doxorubicin-induced cardiotoxicity in human pluripotent stem cell derived-cardiomyocytes. Sci Rep. 2016;6:25333.
29. Fang X, Miao S, Yu Y, Ding F, Han X, Wu H, et al. MIR148A family regulates cardiomyocyte differentiation of human embryonic stem cells by inhibiting the DLL1-mediated NOTCH signaling pathway. J Mol Cell Cardiol. 2019;134:1–12.
30. Lei W, Feng T, Fang X, Yu Y, Yang J, Zhao ZA, et al. Signature of circular RNAs in human induced pluripotent stem cells and derived cardiomyocytes. Stem Cell Res Ther. 2018;9:56.
31. Yu Y, Qin N, Lu XA, Li J, Han X, Ni X, et al. Human embryonic stem cell-derived cardiomyocyte therapy in mouse permanent ischemia and ischemia-reperfusion models. Stem Cell Res Ther. 2019;10:167.
32. Hao K, Lei W, Wu H, Wu J, Yang Z, Yan S, et al. LncRNA-safe contributes to cardiac fibrosis through safe-Sfrp2-HuR complex in mouse myocardial infarction. Theranostics. 2019;9:7282–97.
33. Sharma A, Burridge PW, McKeithan WL, Serrano R, Shukla P, Sayed N, et al. High-throughput screening of tyrosine kinase inhibitor cardiotoxicity with human induced pluripotent stem cells. Sci Transl Med. 2017;9:eaaf2584.
34. Scherer N, Dings C, Bohm M, Laufs U, Lehr T. Alternative treatment regimens with the PCSK9 inhibitors alirocumab and evolocumab: a pharmacokinetic and pharmacodynamic modeling approach. J Clin Pharmacol. 2017;57:846–54.
35. Shitara Y, Sugiyama Y. Pharmacokinetic and pharmacodynamic alterations of 3-hydroxy-3-methylglutaryl coenzyme A (HMG-CoA) reductase inhibitors: drug-drug interactions and interindividual differences in transporter and metabolic enzyme functions. Pharmacol Ther. 2006;112:71–105.
36. Osataphan N, Phrommintikul A, Chattipakorn SC, Chattipakorn N. Effects of doxorubicin-induced cardiotoxicity on cardiac mitochondrial dynamics and mitochondrial function: Insights for future interventions. J Cell Mol Med. 2020;24:6534–57.
37. Kitani T, Ong SG, Lam CK, Rhee JW, Zhang JZ, Oikonomopoulos A, et al. Human-induced pluripotent stem cell model of trastuzumab-induced cardiac dysfunction in patients with breast cancer. Circulation. 2019;139:2451–65.
38. Liang P, Lan F, Lee AS, Gong T, Sanchez-Freire V, Wang Y, et al. Drug screening using a library of human induced pluripotent stem cell-derived cardiomyocytes reveals disease-specific patterns of cardiotoxicity. Circulation. 2013;127:1677–91.
39. Zhao MT, Chen H, Liu Q, Shao NY, Sayed N, Wo HT, et al. Molecular and functional resemblance of differentiated cells derived from isogenic human iPSCs and SCNT-derived ESCs. Proc Natl Acad Sci USA. 2017;114:E11111–20.
40. Kopljar I, De Bondt A, Vinken P, Teisman A, Damiano B, Goeminne N, et al. Chronic drug-induced effects on contractile motion properties and cardiac biomarkers in human induced pluripotent stem cell-derived cardiomyocytes. Br J Pharmacol. 2017;174:3766–79.
41. Raedler LA. Praluent (alirocumab): first PCSK9 inhibitor approved by the FDA for hypercholesterolemia. Am Health Drug Benefits. 2016;9:123–6.
42. Teramoto T, Usami M, Takagi Y, Baccara-Dinet MT, Investigators OJ. Efficacy and safety of alirocumab in japanese patients with diabetes mellitus: post-hoc subanalysis of ODYSSEY Japan. J Atheroscler Thromb. 2019;26:282–93.
43. Bouitbir J, Charles AL, Echaniz-Laguna A, Kindo M, Daussin F, Auwerx J, et al. Opposite effects of statins on mitochondria of cardiac and skeletal muscles: a 'mitohormesis' mechanism involving reactive oxygen species and PGC-1. Eur Heart J. 2012;33:1397–407.
44. Ward NC, Watts GF, Eckel RH. Statin toxicity. Circ Res. 2019;124:328–50.
45. Grundy SM. The issue of statin safety: where do we stand? Circulation. 2005;111:3016–9.
46. Sadighara M, Amirsheardost Z, Minaiyan M, Hajhashemi V, Naserzadeh P, Salimi A, et al. Toxicity of atorvastatin on pancreas mitochondria: a justification for increased risk of diabetes mellitus. Basic Clin Pharmacol Toxicol. 2017;120:131–7.
47. Kaufmann P, Torok M, Zahno A, Waldhauser KM, Brecht K, Krahenbuhl S. Toxicity of statins on rat skeletal muscle mitochondria. Cell Mol Life Sci. 2006;63:2415–25.
48. Nakad A, Bataille L, Hamoir V, Sempoux C, Horsmans Y. Atorvastatin-induced acute hepatitis with absence of cross-toxicity with simvastatin. Lancet. 1999;353:1763–4.
49. Zhang L, Cheng L, Wang Q, Zhou D, Wu Z, Shen L, et al. Atorvastatin protects cardiomyocytes from oxidative stress by inhibiting LOX-1 expression and cardiomyocyte apoptosis. Acta Biochim Biophys Sin. 2015;47:174–82.
50. Tian L, Oikonomopoulos A, Liu C, Kitani T, Shrestha R, Chen CL, et al. Molecular signatures of beneficial class effects of statins on human induced pluripotent stem cell-derived cardiomyocytes. Circulation. 2020;141:1208–10.
51. Feng P, Zhao L, Guo F, Zhang B, Fang L, Zhan G, et al. The enhancement of cardiotoxicity that results from inhibiton of CYP 3A4 activity and hERG channel by berberine in combination with statins. Chem-Biol Interact. 2018;293:115–23.